Revision 1

Synthetic and natural ammonium-bearing tourmaline

Bernd Wunder*[1], Eleanor Berryman[1,2], Birgit Plessen[1], Dieter Rhede[1], Monika Koch-Müller[1], Wilhelm Heinrich[1]

[1]GeoForschungsZentrum Potsdam, 14473 Potsdam, Germany

[2]Fachgebiet Mineralogie-Petrologie, Technische Universität Berlin, 13355 Berlin, Germany

*E-mail: wunder@gfz-potsdam.de

ABSTRACT

Due to the similar ionic radius of K^+ and NH_4^+, K-silicates can incorporate a significant amount of NH_4. As tourmaline is able to accommodate K in its crystal structure at high and ultrahigh pressure, we test if this also holds true for NH_4.

Piston-cylinder experiments in the system $(NH_4)_2O$-MgO-SiO_2-Al_2O_3-B_2O_3-H_2O at 4.0 GPa, 700 °C, with B_2O_3 and NH_4OH in excess produce an assemblage of tourmaline, phengite, and coesite. The tourmaline crystals are up to 10 x 40 μm in size. EMP analyses indicate that the tourmalines contain 0.22 (±0.03) wt% $(NH_4)_2O$ and are solid solutions mainly along the magnesio-foitite and "NH_4-dravite" join with the average structural formula $^X((NH_4)_{0.08(1)}\square_{0.92(1)})^Y(Mg_{2.28(8)}Al_{0.72(8)})^Z(Al_{5.93(6)}Si_{0.07(6)})^T(Si_{6.00(5)}O_{18})(BO_3)_3(OH)_4$. NH_4 incorporation is confirmed by characteristic <N-H> stretching and bending modes in the IR-spectra of single crystals on synthetic tourmaline. Further evidence is the increased unit

cell parameters of the tourmaline (a = 15.9214(9) Å, c = 7.1423(5) Å, V = 1567.9(2) Å^3) relative to pure magnesio-foitite.

Incorporation of NH_4 in natural tourmaline was tested in a tourmaline-bearing mica schists from a high P/ low T (> 1.2 GPa/ 550 °C) meta-sedimentary unit of the Erzgebirge, Germany, rich in NH_4. The NH_4-concentrations in the three main NH_4-bearing phases are: biotite (~1400 ppm) > phengite (~700 ppm) > tourmaline (~500 ppm). This indicates that tourmaline can act as important carrier of nitrogen between the crust and the deep Earth which has important implications for a better understanding of the large-scale light element cycle.

Keywords: Tourmaline, high-pressure synthesis, ammonium, Erzgebirge mica-schists, nitrogen cycle

INTRODUCTION

The transfer of nitrogen from the Earth's surface to its interior occurs by subduction of ammonium-bearing sediments and altered oceanic crust (e.g., Boyd 2001; Hastings et al. 2013; Bebout et al. 2013a; Busigny and Bebout 2013, and references therein). Nitrogen released from organic matter is predominantly incorporated as NH_4^+ into clay minerals during diagenesis and may subsequently substitute for K^+ in K-feldspar, muscovite, biotite and other K-bearing silicates with increasing metamorphic grade (e.g., Williams et al. 1992). There is general agreement that during Barrovian-type metamorphism and during subduction a large proportion of the ammonium is continuously discharged by continuous dehydration reactions (Bebout and Fogel 1992; Bebout et al. 1999; Sadofsky and Bebout 2000; Mingram and Bräuer 2001; Pöter et al. 2004; Pitcairn et al. 2005) and recycled to the surface, for example via arc volcanism. By contrast, high and ultrahigh-pressure, low-temperature metasediments sometimes retain major amounts of NH_4 mainly in micas to at least 3.0 GPa and probably

beyond (Busigny et al. 2003a; Bebout et al. 2013b). In addition, experiments by Watenphul et al. (2009) have shown that the NH_4 analogues of the high-pressure potassium-bearing silicates phengite, K-cymrite, K-hollandite, and K-Si-wadeite are stable to even much higher pressures at relevant temperatures. This indicates that significant amounts of nitrogen can indeed be transported into the deeper mantle. These results are in line with arguments presented by Cartigny and Marty (2013), suggesting that recycling of nitrogen into the mantle presently exceeds outgassing. There is, however, insufficent information about other NH_4-bearing minerals that may contribute to the deep nitrogen cycle, as all K-bearing silicates are potential carriers of nitrogen to depth.

Tourmaline has been long known as carrier of light elements such as boron and lithium in the Earth's crust (e.g., Henry and Dutrow 1996; Busigny and Bebout 2013). It forms in various geochemical environments that have undergone diagenetic, metamorphic, metasomatic, or magmatic processes over a wide range of bulk compositions (van Hinsberg et al. 2011), and has a large pressure and temperature stability field ranging from near-surface (Henry et al. 1999) to mantle conditions (Krosse 1995; Marschall et al. 2009). Tourmaline has a very flexible structure, which is able to adjust its composition in response to a wide range of chemical, pressure and temperature variations (Dutrow and Henry 2011) as reflected by its complex general chemical formula, $XY_3Z_6[T_6O_{18}](BO_3)_3V_3W$ (Hawthorne and Henry 1999). The large X site is nine-fold coordinated and typically contains Na, Ca and vacancies (□) in varying amounts (Hawthorne and Dirlam 2011). K-rich tourmalines are rare (Marschall et al. 2009); however, K-dominant tourmalines with up to 0.6 K per formula unit (pfu) have been reported (Grice et al. 1993; Žáček et al. 2000; Shimizu and Ogasawara 2005; 2013).

Recent experimental studies at various pressure and temperature (*P*-*T*) conditions have shown that in the system MgO-Al_2O_3-SiO_2-B_2O_3-KCl-(NaCl)-H_2O tourmaline may incorporate up to 0.71 K pfu, provided that the pressure is high enough (4.0 GPa, 700 °C) and the bulk composition Na-poor (Berryman et al. 2014; and in prep.). For Na-free bulk

compositions, these synthetic tourmalines are mainly solid solutions between the end-member compositions of K-dravite [$KMg_3Al_6Si_6O_{18}(BO_3)_3(OH)_3(OH)$], Mg-foitite [$\square(Mg_2Al)Al_6(Si_6O_{18})(BO_3)_3(OH)_3(OH)$], and K-olenite [$KAl_3Al_6Si_6O_{18}(BO_3)_3O_3(OH)$]. Since high pressure encourages the incorporation of K^+, this may also hold for the similarly-sized ammonium ion, NH_4^+.

In this contribution, we test whether high-pressure tourmaline is a potential host for nitrogen by performing experiments in a piston-cylinder apparatus. We will show that magnesio-foitite can accommodate an "NH_4-dravite" component up to 8 mole% at 4.0 GPa, 700 °C, indicating that tourmaline can transport nitrogen from the Earth's crust into the mantle. We also measure the nitrogen concentrations in tourmaline coexisting with white mica and biotite from a well-known nitrogen-bearing high-pressure metasedimentary unit of the Erzgebirge (Germany), whose whole-rock nitrogen concentration is ~ 400 ppm (Mingram and Bräuer 2001). Data on NH_4-partitioning between micas and tourmaline will demonstrate that tourmaline may constitute a reservoir of nitrogen in metamorphic rocks. We argue that tourmaline is not only important in the transport of boron and lithium but also of nitrogen during large-scale long-term cycling of light elements in subduction processes.

EXPERIMENTAL AND ANALYTICAL METHODS

Experimental procedure

NH_4-bearing tourmaline was synthesized at 4.0 GPa, 700 °C with a 5-days run duration in a piston-cylinder press. The solid starting material consisted of a homogeneous mixture of SiO_2, γ-Al_2O_3, MgO, and H_3BO_3 in the stoichiometric proportions of end-member dravite, $NaMg_3Al_6Si_6O_{18}(BO_3)_3(OH)_4$, without any sodium, and with excess SiO_2 and H_3BO_3. Following the method of tourmaline synthesis from previous studies (von Goerne and Franz 2000; Meyer et al. 2008; Berryman et al. 2014) we used excess boric acid in double of the stoichiometric amounts, and excess SiO_2 by 20 mole% to compensate for high fluid solubility

of these components. About 15 mg of the solid starting material was loaded into a welded gold capsule 10 mm in length and 3 mm in diameter together with ~3 mg of a 25% $NH_4(OH)$ solution. The capsule was placed into a high-pressure cell consisting of a steel furnace with fired pyrophyllite and rock salt as pressure media. The pressure uncertainty of this assembly is approximately 1%, calibrated according to the quartz-coesite transition (Mirwald and Massonne 1980). Pressure was maintained within 50 MPa throughout the experiment. The temperature was monitored using a Ni-CrNi thermocouple; its error is estimated to be ±10 °C. At the end of the experiment, the sample was quenched isobarically in less than 15 seconds below 200 °C prior to the slow release of pressure. The capsule was cleaned and reweighed to check for leakage. The smell of ammonia upon opening the capsule indicated that ammonium was available in excess throughout the experiment. The solid product was removed from the capsule and prepared for X-ray powder diffraction, scanning electron microscopy, infrared-analyses and electron microprobe analyses.

Analytical methods

X-ray diffraction (XRD). Powder XRD analysis was performed with a Stoe Stapid P diffractometer operated at 40 kV and 40 mA using Cu$K\alpha_1$ radiation collected in the 2θ range 5° to 125° with a detector step size of 0.1°, a 2θ resolution of 0.01°, and counting times of up to 20 s per step. Structural parameter and phase proportions were constrained using the GSAS software package for Rietveld refinement (Larson and Von Dreele 2004). The initial structure models were taken from the Inorganic Structure Database (ICSD, FIZ Karlsruhe). For tourmaline, we used the structural input parameters of dravite (Buerger et al. 1962), modified according to the EMP-determined site occupancies and substituting Na for NH_4 at the X-site based on their identical number of electrons.

Infrared (IR) spectroscopy. Prior to the IR-analyses, the run product was washed in distilled water to remove any remaining boric acid and $NH_4(OH)$ from the sample surface. IR-measurements were performed on a few approximately 10 μm wide and 40 μm long tourmaline single crystals, which were handpicked under a binocular microscope. We took care to ensure that no mica was attached to the surface of the selected tourmalines. Using a piston-cylinder type diamond-anvil cell (DAC), the tourmaline crystals were pressed into a 2 - 3 μm thin film. IR measurements were conducted with a Vertex 80 v FTIR spectrometer connected to a Hyperion microscope using a Globar light source, a KBr beam splitter, and a MCT detector. Spectra were collected in the 4000 - 500 cm^{-1} spectral range with a resolution of 2 cm^{-1}, averaged over 256 scans. Absorbance features from the diamond occur in the 2400-1800 cm^{-1} spectral range (Fig. 3, *see* below).

The FTIR detection limit for nitrogen incorporation in silicates is difficult to estimate as it depends on the sharpness of the N-H bands, on the thickness of the sample and the degree of band overlap. The strongest N-relating IR band is the <N-H>-bending band ν_4 (see below) and we estimate the detection limit for N based on this vibration in the 2 – 3 μm thin films to about 100 - 150 ppm N.

Electron microprobe (EMP) analyses of experimental products. EMP-analyses were performed on washed, epoxy-mounted, polished, and carbon-coated grain mounts. Wavelength dispersive electron microprobe analyses were carried out using a JEOL JXA-8230 SuperProbe equipped with a LaB_6 cathode and five spectrometers. The analytical conditions were: 15 kV acceleration voltage, 20 nA beam current and 5 μm beam diameter. Natural silicates were used as standards for Si, Al (plagioclase) and Mg (diopside). Boron was not analyzed. Counting times on the signal peaks were 20 seconds for Mg, and 10 seconds for Si and Al. The background counting times were always set to the half of the respective peak counting times. The raw intensity data were corrected with the Armstrong CITZAF on-line

155 correction program (Armstrong, 1995). Nitrogen (N-Kα-line) was quantified using a layered
156 dispersion analyzing crystal [LDE5H-(*Cr/Sc*)] with a 2d spacing of 80 Å and two different N-
157 standards with different N-contents and N-bonding matrices: (a) natural NH_4-bearing phengite
158 and (b) synthetic boron nitride.

159 The NH_4-bearing phengite, which was used as N-standard in the EMP-analyses, comes
160 from an Erzgebirge mica schist (sample # 61, further characterization given below). The NH_4
161 content of this phengite was carefully determined by two independent methods, which were
162 described in detail by Mingram and Bräuer (2001) and Plessen et al. (2010). Prior to analysis,
163 separated phengite crystals (up to 1 mm in diameter) were ground to < 63 μm in an agate
164 mortar. After being dried at 110 °C, approximately 30 mg of the sample powder was loaded
165 into tin capsules and measured for (i) total nitrogen using an elemental analyzer NA1500
166 coupled via a ConFlow II with an isotopic ratio mass spectrometer (IRMS) $DELTA_{plus}XL$
167 (ThermoFischer); for the extraction of (ii) NH_4^+- nitrogen the HF-digestion and distillation
168 techniques were used (Plessen et al. 2010). Approximately 200 to 500 mg of dried sample
169 was weighed into polypropylene bottles and then digested using 5 ml of 40 % HF and 1 ml
170 0.1 N H_2SO_4. After digestion, a 20 % KOH solution was added to raise the pH, and the whole
171 solution was distilled using a Kjeldahl apparatus until 20 ml of distillate has been collected in
172 10 ml 0.01 N H_2SO_4 solution. The amount of fixed-nitrogen (NH_4^+-N) was determined by
173 titration using 0.01 N NaOH, with N-yields of 5 - 15 μg. The possibility of N-contamination
174 was tested with one blank sample per batch. The nitrogen concentrations in eight different
175 phengite samples determined by method (i) ranged from 651 to 705 ppm N_{tot}, with a mean
176 value of 678 (±22) ppm. Nitrogen concentrations (six samples) via method (ii) range from
177 638 to 819 ppm, with a mean value of 735 (±62) ppm. EMP scanning of phengites from thin
178 sections of the sample confirmed that they are homogeneous with respect to their nitrogen
179 contents. In order to use these phengite crystals as EMP standards, we set the nitrogen

concentration to be 700 (±40) ppm, which is about the mean N-concentation determined by the two analytical methods, and which corresponds to 0.27 (±0.02) wt% $(NH_4)_2O$.

EMP determination of the same phengites in thin section using boron nitride as standard resulted in apparent nitrogen concentrations of 0.81 (±0.11) wt% $(NH_4)_2O$. Similarly, BN-based EMP analyses of biotite (wet chemical analyses given in Plessen et al. 2010) gave apparent concentrations that are too high by a factor of three. We therefore conclude that boron nitride is an inappropriate nitrogen standard for EMP analyses of silicates and dismissed these values. Instead, we rely on the well-characterized natural phengite for nitrogen standardization. EMP data of the synthetic tourmaline were normalized to 15 cations at the Y, Z, and T sites assuming 3 B pfu.

EMP analyses of NH_4-bearing tourmaline, phengite, and biotite from the Erzgebirge mica schist. EMP analyses were performed on polished thin sections using the same instrument as described above. The analytical conditions were: 15 kV accelaration voltage, 20 nA beam current, and 20 μm beam diameter. Element standards were mostly natural silicates and oxides: Na: albite; Si, Al: plagioclase; Ca, Mg: diopside; K: orthoclase; Ti: rutile; Fe: Fe_2O_3; F: fluorite; Mn: rhodonite; Ba: $BaSi_2O_5$; Cl: tugtupite. Boron was not analyzed. As was done for the synthetic tourmaline, the natural NH_4-bearing phengite (# 61) was used as a standard for the nitrogen analyses in tourmaline and mica. Counting times on the signal peaks were: 10 seconds for Na, Si, and Al; 40 seconds for N; and 20 seconds for the other elements. Due to the long counting time for nitrogen, we estimate the detection limit (2σ) to be below 160 ppm N. The background counting times on each side of the peak were always half of the peak counting times. The EMP data of natural tourmaline were normalized to 15 cations at the Y, Z, T sites, assuming 3 B pfu and total iron as Fe^{2+}. Data of the natural micas were normalized to 11 oxgens and total iron was assumed to be ferrous.

206 **Sample from the Erzgebirge, Germany**

207 Whole-rock ammonium concentrations and nitrogen isotope compositions in
208 metasediments from different tectonometamorphic units in the European Variscan Belt have
209 been studied in detail by Mingram and Bräuer (2001), however, NH_4-concentrations of
210 individual minerals were not given. For our study, we chose a tourmaline-bearing, feldspar-
211 free mica schist of the mica schist/eclogite unit, which has a NH_4 whole-rock concentration of
212 390 ppm (sample # 61; Mingram and Bräuer (2001), their Table 3). This assemblage consists
213 of phengite + chloritoid + quartz + garnet ± biotite ± chlorite ± tourmaline, equilibrated at
214 about 1.2 GPa/ 550 °C (Mingram and Bräuer (2001); their Table 2). The tourmaline are of
215 brownish colour, unzoned and often surrounded by mica indicating synmetamorphic
216 formation. We carefully selected thin sections with closely associated tourmaline, phengite,
217 and biotite crystals, aiming at deriving reliable values of NH_4-partitioning among these
218 phases.

219

220 **RESULTS**

221 **Synthetic NH_4-bearing tourmaline**

222 The experiments produced a mixture of tourmaline (60 wt%), mica (39 wt%, mainly
223 of the $2M_1$ polytype), and traces of coesite as determined from quantitative phase analysis of
224 the XRD-measurement. The refined cell-dimensions of the NH_4-bearing tourmaline are: a =
225 15.9214(9) Å, c = 7.1423(5) Å, V = 1567.9(2) Å^3. We compare these values with those of
226 end-member dravite (Buerger et al. 1962) and various tourmalines synthesized in the system
227 SiO_2-Al_2O_3-MgO-B_2O_3-H_2O, but with different X-site-occupying cations (Fig. 1). Both the a
228 and c dimensions of our NH_4-bearing tourmaline are significantly larger than those of Mg-
229 foitite [$\square(Mg_2Al)Al_6(Si_6O_{18})(BO_3)_3(OH)_4$], ($a$ = 15.90 Å, c = 7.115 Å, Werding and Schreyer
230 1984), in which the X-site is completely vacant, indicating a distinct NH_4-component at the
231 X-site. The ionic radius of $^{[9]}NH_4^+$ = (1.60 Å; Gottschalk, personal communication 2014) is

232 slightly larger than $^{[9]}K^{+}$ (1.55 Å; Shannon 1976). The smaller cell-dimensions of our
233 tourmaline compared to those of K-bearing tourmaline (a = 15.927 Å; c = 7.193 Å, Berryman
234 et al. 2014) with □ = 0.41 (Fig. 1) reflects that the amount of NH_4^+ at the X-site is
235 significantly smaller than 0.6 pfu. Furthermore, in an undistorted tetrahedron, the ideal $<^{T}$Si-
236 O> bond length is 1.62 Å, a value that strongly differs from the bond length of 1.47 Å
237 predicted for $<^{T}$B-O> (Hawthorne 1996). The mean <T-O>-distance determined by the
238 Rietveld refinement of tourmaline is 1.623(35) Å, indicating complete occupancy of the T-site
239 by Si. This excludes the presence of $^{[4]}$B as being responsible for the decrease in cell-
240 dimensions (Schreyer et al. 2000) and confirms the absence of tetrahedrally coordinated
241 boron in our synthetic tourmalines.
242 Lattice parameters for the most abundant polytype of mica ($2M_1$) are a = 5.256(4) Å, b
243 = 8.865(6) Å, c = 20.18(1) Å, β = 93.6(1)°, V = 938.5(9) Å^3. Compositional data are not
244 available, however, based on the experimental conditions these micas are phengites (Melzer
245 and Wunder 2000) and probably NH_4-bearing. Their cell-volume is significantly smaller than
246 that of synthetic $2M_1$-NH_4-phengite (V = 960.9 Å^3, Watenphul et al. 2009) and larger than
247 that of synthetic $2M_1$-boromuscovite (V = 873.7 Å^3, Wunder et al. 2005). One may interpret
248 that our phengites might have a significant NH_4-boromuscovite component, and/or that the
249 $^{[12]}$X-site is not completely filled by NH_4, i.e., a pyrophyllite component might be present.
250
251 The synthesized tourmaline crystals have dimensions up to 10 x 40 μm and are
252 generally idiomorphic, prismatic, and often form radially grown aggregates (Fig. 2). The
253 micas are much smaller (< 5 μm in diameter, < 1 μm in thickness) and not suitable for reliable
254 EMP-analyses.
255

The IR spectrum of synthetic tourmaline is shown in Figure 3 along with the IR-spectrum of a natural NH_4-free schorl (Salisbury et al. 1991). Differences in the IR-spectra are the additional bands at 3650, 3320, 3060, 1460, 1420 and 1370 cm^{-1} occurring only for the synthetic tourmaline. Following e.g., Busigny et al. (2003b), Watenphul et al. (2009), the bands at 3320 and 3060 cm^{-1} correspond to <N-H>-stretching (ν_3 and $2\nu_2$ according to Watenphul et al. (2009), their Table 4). The three bands between 1460 – 1370 cm^{-1} are assigned to <N-H>-bending (Busigny et al. 2003b) and correspond to ν_4 and further overtone and combination modes (Watenphul et al. (2009), their Table 4). The band at 3650 cm^{-1} is an <O-H>-stretching vibration, which results from vacancies at the X-position (Fantini et al. 2014) and which has also been observed in the IR-spectra of synthetic alkali-free tourmaline (i.e., Mg-foitite; Rosenberg and Foit 1979). The assignments of the IR stretching and bending bands are summarized in Table 1.

It is very likely that the mica occurring in the reaction product incorporated NH_4. Thus, carefully washed and hand-selected tourmaline crystals were used. The strongest <N-H>-stretching and -bending bands of NH_4-bearing phengite occur at 3311 and 1433 cm^{-1}, respectively (Watenphul et al. 2009). As these bands do not appear in our spectrum (Fig. 3), we can confidently exclude that the measured NH_4-bands result from the presence of NH_4-bearing mica. The IR spectrum of our synthetic tourmalines gives clear evidence for structural incorporation of NH_4 in tourmaline. In addition, no <O-H>-band is observed at 3367 cm^{-1}, the presence of which would indicate tetrahedrally-coordinated boron (Schreyer et al. 2000). This is in line with measured mean <T-O>-distances from XRD-analysis (see above) and confirms the absence of tetrahedrally-coordinated boron in our synthetic tourmalines.

The chemical composition of the synthetic tourmaline (n = 49) is given in Table 2, along with the recalculated structural formula. As discussed above, the measured nitrogen concentrations depend on the reliability of the natural NH_4-bearing phengite as nitrogen

standard. Recalculated nitrogen concentrations give 0.22 (±0.03) wt% $(NH_4)_2O$, corresponding to an X-site occupancy of 0.08 (±0.01) NH_4^+ after normalization to 15 YZT cations and assuming 3 B pfu. The average structural formula is $^{[X]}((NH_4)_{0.08(1)}\square_{0.92(1)})^{[Y]}(Mg_{2.28(8)}Al_{0.72(8)})^{[Z]}(Al_{5.93(6)}Si_{0.07(6)})^{[T]}(Si_{6.00(5)}O_{18})(BO_3)_3(OH)_4$. This tourmaline is basically a solid solution between the end-members magnesio-foitite $[\square(Mg_2Al)Al_6(Si_6O_{18})(BO_3)_3(OH)_3(OH)]$ and NH_4-dravite $[NH_4Mg_3Al_6Si_6O_{18}(BO_3)_3(OH)_3(OH)]$. It has a very small component of octahedral $^{[Z]}Si$ (0.07 pfu), which may result from its formation at ultrahigh-pressure. Octahedral silicon has been previously observed in olenitic tourmaline synthesized at high pressure (Schreyer et al. 2000). EMP-analyses on the coexisting NH_4-bearing micas, presumably phengitic, did not produce reliable data due to their small crystal size.

Natural tourmaline from the high *P*/low *T* mica schist, Erzgebirge, Germany

Compositions of three tourmalines from a thin section of this rock are presented in Table 3. Again, nitrogen concentrations were obtained using the natural phengite reference sample (# 61) as described above. Within analytical errors the three tourmaline crystals have identical nitrogen concentrations of ~500 ppm N. Assuming the measured nitrogen is ammonium, the mean X-site occupancy of these natural tourmalines is calculated as 0.08 (±0.01) NH_4 pfu, coincidentally, the same amount as detected in the simplified (Na, Ca, and Fe-free) experimental system used above. The three tourmalines are compositionally homogeneous, unzoned and have nearly identical compositions.

The structural formula is:

$^{[X]}((NH_4)_{0.08(1)}Na_{0.72(5)}Ca_{0.01(0)}K_{0.01(0)}\square_{0.18(5)})$

$^{[Y]}(Mg_{1.67(9)}Fe_{1.12(3)}Al_{0.21(9)})$

307 $^{[Z]}(Al_{5.73(9)}Ti_{0.09(2)}Si_{0.18(2)})^{[T]}(Si_{6.00(2)}O_{18})(BO_3)_3$

308 $^{[V]}(OH)_{3.00(3)}{}^{[W]}((OH)_{0.68(3)}O_{0.31(4)}F_{0.01(0)}$

309 They are Ca-free and mainly a solid solution of the dravite

310 $[NaMg_3Al_6Si_6O_{18}(BO_3)_3(OH)_3(OH)]$, (Mg,Fe)-foitite [□

311 $(Mg,Fe)_2Al)Al_6(Si_6O_{18})(BO_3)_3(OH)_3(OH)]$, and olenite $[NaAl_3Al_6Si_6O_{18}(BO_3)_3O_3(OH)]$ end-

312 member compositions, containing 8 mole% of a NH_4-dravite component. The tourmalines are

313 aluminous, reflecting the metapelitic nature of the host rock, and are very Si-rich with 6.18

314 (±0.18) Si pfu. Again, incorporation of Si into the octahedrally coordinated Z-site probably

315 results from the high pressure formation conditions of these rocks (Schreyer et al. 2000).

316 Compositional details (disregarding nitrogen) of phengite and biotite from this sample

317 were given by Rötzler et al. (1998) and used for phengite barometry as well as for garnet-

318 phengite and garnet-biotite thermometry (see also Willner et al. 1997). We re-analyzed some

319 of the biotites and phengites by EMP with particular emphasis on their NH_4-concentrations.

320 The phengite $((NH_4)_{0.04(1)}K_{0.84(3)}Na_{0.05(2)})_{0.93}$ $(Al_{1.7(1)}Ti_{0.01(0)}Mg_{0.2(1)}Fe_{0.14(2)})$ $(Al_{0.7(1)}Si_{3.3(1)}O_{10})$

321 $(F_{0.03(2)}(OH)_{1.97})$ (n = 81) and

322 biotite $((NH_4)_{0.09(1)}K_{0.7(2)}Na_{0.01(0)}Ca_{0.01(0)})_{0.81}$ $(Mg_{0.8(1)}Fe_{1.5(1)}Al_{0.53(3)}Ti_{0.06(1)})_{2.9}$

323 $(Si_{2.7(2)}Al_{1.3(1)}O_{10})$ $(F_{0.07(3)}(OH)_{1.93})$ (n = 10)

324 compositions agree with previous data given in Rötzler et al. (1998). Our added values for the

325 NH_4 concentrations, recalulated to parts per million in the respective phases, give ~1400 ppm

326 NH_4 in biotite and ~700 ppm NH_4 in phengite on average. Assuming that Henry's law for

327 equilibrium distribution is valid for these low concentrations, partition coefficients in terms of

328 $D_{NH4}^{phase1-phase2} = \frac{C_{NH4}^{phase1}}{C_{NH4}^{phase2}}$ are calculated, resulting in $D_{NH4}^{tur-phg} \approx 0.7$ and $D_{NH4}^{tur-bt} \approx 0.4$ at the relevant

329 conditions of 550 °C/12 kbar. D_{NH4}^{bt-phg} is 2, broadly in line with experimental results on NH_4-

330 partitioning between muscovite and NH_4-bearing fluid (Pöter et al. 2004) and between

331 phlogopite and NH_4-bearing fluid (Bos et al. 1988) performed between 500 and 600 °C at 0.1

to 0.4 GPa. Combining the results indicates that at low NH_4-concentrations, phlogopite incorporates about 2-3 times as much NH_4 as muscovite. Comparable distributions in natural NH_4-bearing micaschists were previously reported (e.g., Boyd and Philippot 1998; Sadofsky and Bebout 2000). This suggests that equilibrium partitioning of NH_4 in these Erzgebirge rocks was attained.

DISCUSSION

Tourmaline has the ability to incorporate a wide variety of elements as mono-, di-, tri-, and tetravalent cations (Dutrow and Henry 2011). We have demonstrated that tourmaline can accommodate significant amounts of NH_4^+, the ammonium ion, thereby adding nitrogen to the long list of possible main elements in tourmaline's complex structure. Although we have shown this for tourmaline formed at high-pressure metamorphic conditions, it is possible that it also applies for tourmaline formed in diagenetic, low and high *P-T* hydrothermal, and even in magmatic environments. Any nitrogen-bearing fluid-rock system at sufficiently reducing conditions may contain or produce NH_4, which, due to its similar ionic radius to Rb, may to certain extent replace the larger monovalent cations such as K, in most silicate structures, particularly in micas and K-feldspar. In contrast, experiments by Berryman et al. (2014; and in prep.) have shown that significant K-incorporation into tourmaline is restricted to high pressure conditions and K-rich, Na-poor bulk compositions. This might also hold true for NH_4 and in this respect, significant NH_4-concentration in tourmaline may indicate formation at high pressure. Further support is gained by NH_4-equilibrium distributions in the tourmaline-bearing Erzgebirge micaschists ($D_{NH4}^{tur-phg} \approx 0.7$ and $D_{NH4}^{tur-bt} \approx 0.4$) where the three main NH_4-bearing phases are biotite (~1400 ppm NH_4), phengite (~700 ppm NH_4) and tourmaline (~500 ppm NH_4). One may reasonably assume that the NH_4-distribution are pressure and temperature dependent, resulting in distinctly different partition coefficients across the large range of *P-T* conditions where biotite, phengite and tourmaline form stable assemblages.

Empirical and experimental calibrations for verification of such a potential geo-thermo/barometer are required for that.

The composition of tourmaline's X-side provides compositional information about the crystallizing fluid. The experimental determination of partition coefficients allows us to extract this information from a tourmaline crystal. However, an important distinction between the experiments and the natural rocks is that the natural tourmaline crystallized from a fluid containing a variety of X-site-occupying cations (i.e., Na, K, Ca, NH_4), whereas our experiments only had NH_4^+. This means that our experimental system prevented any competition for X-site occupancy. Nonetheless, the similar NH_4 content of our synthetic and natural tourmaline suggests that tourmaline can incorporate a limited amount of the large NH_4 ion into its structure. This has to be proven by additional experiments at different *P*-*T*-X conditions.

The upper pressure stability of dravitic tourmaline relevant to subduction zone conditions is around 7 GPa (Krosse 1995) and tourmaline has been reported to occur in many high and ultrahigh pressure rocks (Marschall et al. 2009). Tourmaline has been shown to serve as a unique indicator for the geochemical cycle of light elements, such as boron and lithium in subduction zones. In particular, tourmaline's boron isotope composition has been extensively used for deciphering fluid transport and fluid-rock interactions during various stages of prograde and retrograde metamorphism occuring within a subduction channel and beyond (Marschall and Jiang 2011). Similarly, its capacity to incorporate NH_4 turns tourmaline into a potential tracer of nitrogen cycling in subducting slabs. In regard to large-scale long-term cycling of light elements between crust and deep Earth, tourmaline is not only an important carrier of boron, but also of nitrogen.

IMPLICATIONS

In our study we show that tourmaline can incorporate significant amounts of nitrogen, in the form of NH_4, into its crystal structure. The feasibility of such a large molecule to be incorporated on the X-position of tourmaline is of crystallographic interest and might initiate further studies concerning the NH_4-bearing tourmaline's crystal structure, including the determination of the NH_4-orientation in the tourmaline structure.

Boron and nitrogen are generally associated in oceanic pelagic sediments thereby leading to the formation of NH_4-bearing borosilicate tourmaline. Our finding will encourage future studies to measure nitrogen in natural tourmaline, particularly in meta-sedimentary samples. We show that tourmaline, in combination with its stability to high pressure, can act as important carrier of nitrogen between the crust and the deep Earth. This has important implications for a better understanding of the large-scale light element cycle. In this context, measuring nitrogen and boron isotopes in NH_4-bearing tourmalines and the above-mentioned investigations on *P*- and *T*-dependent ammonium partition coefficients between tourmaline and mica have a strong potential for advanced studies.

ACKNOWLEDGEMENTS

H.-P. Nabein and U. Dittmann for sample preparation, O. Appelt for EMP- and I. Schäpan for SEM-measurements. Thoughtful reviews by G.E. Bebout and V. van Hinsberg improved the final version of the manuscript. A DFG grant to G. Franz and W.H. (FR 557/ 31-1; HE 2015/16-1) and a NSERC scholarship to E.B. are gratefully acknowledged.

REFERENCES CITED

Armstrong, J.T. (1995) CITZAF: a package of correction programs for the quantitative electron microbeam X-ray-analysis of thick polished materials, thin films, and particles. Microbeam Analysis, 4, 177-200.

Bebout, G.E., Fogel, M.L., and Cartigny, P. (2013a) Nitrogen: Highly volatile yet surprisingly compatible. Elements, 9, 333-338.

Bebout, G.E., Agard, P., Kobayashi, K., Moriguti, T., and Nakamura, E. (2013b) Devolatilization history and trace element mobility in deeply subducted sedimentary rocks. Evidence from western Alps HP/UHP suites. Chemical Geology, 342, 1-20.

Bebout, G.E., Cooper, D.C., Bradley, A.D., and Sadofsky, S.J. (1999) Nitrogen-isotope record of fluid-rock interactions in the Skiddaw aureole and granite, English Lake District. American Mineralogist, 84, 1495-1505.

Bebout, G.E., and Fogel, M.L. (1992) Nitrogen-isotope compositions of metasedimentary rocks in the Catalania schists, California: Implications for metamorphic devolatization history. Geochimica et Cosmochimica Acta, 56, 2839-2848.

Berryman, E., Wunder, B., and Rhede, D. (2014) Synthesis of K-dominant tourmaline. American Mineralogy, 99, 539-542.

Bos, A., Duit, W., Van der Erden A.M.J., and Jansen, J.B.H. (1988) Nitrogen storage in biotite: An experimental study of the ammonium and potassium partitioning between 1M-phlogopit and vapour at 2 kb. Geochimica et Cosmochimica Acta, 52, 1275-1283.

Boyd, S.R. (2001) Nitrogen in future biosphere studies. Chemical Geology, 176, 1-30.

Boyd, S.R., and Philippot, P. (1998) Precambrium ammonium biogeochemistry: A study of the Moine metasediments, Scotland. Chemical Geology, 144, 257-268.

Buerger, M.J., Burnham, C.W., and Peacor, D.R. (1962) Assessment of the several structures proposed for tourmaline. Acta Crystallographica, 15, 483-490.

Busigny, V., and Bebout, G.E. (2013) Nitrogen in the silicate Earth: speciation and isotopic behavior during mineral-fluid interactions. Elements, 9, 353-358.

Busigny, V., Cartigny, P., Philippot, P., Ader, M., and Javoy, M. (2003a) Massive recycling of nitrogen and other fluid-mobile elements (K, Rb, Cs, H) in a cold slab environment:

evidence from HP to UHP oceanic metasediments of the Schistes Lustrés nappe (western Alps, Europe). Earth and Planetary Sciences Letters, 215, 27-42.

Busigny, V., Cartigny, P., Philippot, P., and Javoy, M. (2003b) Ammonium quantification in muscovite by infrared spectroscopy. Chemical Geology, 198, 21-31.

Cartigny, P., and Marty, B. (2013) Nitrogen isotopes and mantle geodynamics: The emergence of life and the atmosphere-crust-mantle connection. Elements, 9, 359-366.

Dutrow, B.L., and Henry, D.J. (2011) Tourmaline: A geologic DVD. Elements, 7, 301-306.

Fantini, C., Tavares, M.C., Krambrock, K., Moreira, R.L., and Righi, A. (2014) Raman and infrared study of hydroxyl sites in natural uvite, fluor-uvite, magnesio-foite, dravite and elbaite tourmalines. Physics and Chemistry of Minerals, 41, 247-254.

Gonzales-Carreño, T. Fernández, M., and Sanz, J. (1988) Infrared and electron microscope analysis of tourmalines. Physics and Chemistry of Minerals, 15, 452-460.

Grice, J.D., Ercit, T.S., and Hawthorne, F.C. (1993) Povondraite, a redefinition of the tourmaline ferridravite. American Mineralogist, 78, 433-436.

Hawthorne, F.C. (1996) Structural mechanisms for light-element variations in tourmaline. Canadian Mineralogist, 34, 123-132.

Hawthorne, F.C., and Dirlam, D.M. (2011) Tourmaline the indicator mineral: From atomic arrangement to viking navigation. Elements, 7, 307-312.

Hawthorne, F.C., and Henry, D.J. (1999) Classification of the minerals of the tourmaline group. European Journal of Mineralogy, 11, 201-215.

Hastings, M.G., Casciotti, K.L., and Elliott, E.M. (2013) Stable isotopes as tracers of anthropogenic nitrogen sources, deposition, and impacts. Elements, 9, 339-344.

Henry, D.J., Kirkland, B.L., and Kirkland, D.W. (1999) Sector-zoned tourmaline from the cap rock of a salt dome. European Journal of Mineralogy, 11, 263-280.

457 Henry, D.J., and Dutrow, B.L. (1996) Metamorphic tourmaline and its petrologic
458 applications. In: Grew, E.S., and Anovitz, L.M. (eds.) Boron: Mineralogy, Petrology
459 and Geochemistry. Reviews in Mineralogy. 33, 503-557.
460 Jagannadha Reddy, B., Frost, R.L., Martens, W.N., Wain, D.L., and Kloprogge, J.T. (2007)
461 Spectroscopic characterization of Mn-tourmalines. Vibrational Spectroscopy, 44(1),
462 42-49.
463 Krosse, S. (1995) Hochdrucksynthese, Stabilität and Eigenschaften der Borsilikate Dravit und
464 Kornerupin sowie Darstellung und Stabilitätsverhalten eines neuen Mg-Al-Borates.
465 Unpublished Doctor´s thesis, Ruhr-Universität Bochum, 131 pp.
466 Larson, A.C., and Von Dreele, R.B. (2004) Generalized structure analysis system. Los
467 Alamos National Laboratory Report LA-UR-86-748.
468 Marschall, H.R., Korsakov, A.V., Luvizotto, G.L., Nasdala, L., and Ludwig, T. (2009) On the
469 occurrence and boron isotopic composition of tourmaline in (ultra)high-pressure
470 metamorphic rocks. Journal of the Geological Society, London, 166, 811-823.
471 Marschall, H.R., and Jiang, S.-Y. (2011) Tourmaline isotopes: No element left behind.
472 Elements, 7, 313-319.
473 Melzer, S., and Wunder, B. (2000) Island-arc basalt alkali ratios: Constraints from phengite-
474 fluid partitioning experiments. Geology, 28, 7, 583-586.
475 Meyer, C., Wunder, B., Meixner, A., Romer, R.L., and Heinrich, W. (2008) Boron-isotope
476 fractionation between tourmaline and fluid: an experimental re-investigation.
477 Contributions to Mineralogy and Petrology, 156, 259-267.
478 Mingram, B., and Bräuer, K. (2001) Ammonium concentration and nitrogen isotope
479 composition in metasedimentary rocks from different tectonometamorphic units of the
480 European Variscan Belt. Geochimica et Cosmochimica Acta, 65, 2, 273-287.
481 Mirwald, P.W., and Massonne, H.-J. (1980) Quartz-coesite transition and the comparative
482 friction measurements in piston-cylinder apparatus using talc-alsimag-glass (TAG)

and NaCl high pressure cells: a discussion. Neues Jahrbuch Mineralogische Monatshefte, 1980, 469-477.

Pitcairn, I.K., Teagle, D.A.H., Kerrich, R., Craw, D., and Brewer, T.S. (2005) The behaviour of nitrogen and nitrogen isotopes during metamorphism and mineralization: Evidence from Otago and Alpine schists, New Zealand. Earth and Planetary Science Letters, 233, 229-246.

Plessen, B., Harlov, D., Henry, D., and Guidotti, C.V. (2010) Ammonium loss and nitrogen isotopic fractionation in biotite as a function of metamorphic grade in metapelites from western Maine, USA. Geochimica et Cosmochumica Acta, 74, 16, 4759-4771.

Pöter, B., Gottschalk, M., and Heinrich, W. (2004) Experimental determination of the K-NH_4-partitioning between muscovite, K-feldspar, and aqueous chloride solutions. Lithos, 74, 67-90.

Rosenberg, P.E., and Foit Jr., F.F. (1979) Synthesis and characterization of alkali-free tourmaline. American Mineralogist, 64, 180-186.

Rötzler, K., Schumacher, R., Maresch, V.W., and Willner, A.P. (1998) Characterization and geodynamic implications of contrasting metamorphic evolution in juxtaposed high-pressure units of the western Erzgebirge (Saxonia, Germany). European Journal of Mineralogy, 10, 261-280.

Sadofsky, S.J., and Bebout, G.E. (2000) Ammonium partitioning and nitrogen-isotope fractionation among coexisting micas during high-temperature fluid-rock interactions: Examples from the New England Appalachians. Geochimica et Cosmochimica Acta, 64, 2835-2849.

Salisbury, J.W., Walter, L.S., Vergo, N., and D'Aria, D.M. (1991) Infrared (2.1-25 μm) spectra of minerals. The John Hopkins University Press, Baltimore, 276 pp.

Schreyer, W., Wodara, U., Marler, B., Van Aken, P.A., Seifert, F., and Robert, J.-L. (2000) Synthetic tourmaline (olenite) with excess boron replacing silicon in the tetrahedral

site: I. Synthesis conditions, chemical and spectroscopic evidence. European Journal of Mineralogy, 12, 529-541.

Shannon, R.D. (1976) Revised ionic radii and systematic studies of interatomic distances in halides and chalcogenides. Acta Crystallographica, A32, 751-767.

Shimizu, R.. and Ogasawara, Y. (2005) Discovery of K-tourmaline in diamond-bearing quartz-rich rock from the Kokchetav Massif, Kazakhstan. Mitteilungen der Österreichischen Mineralogischen Gesellschaft, 150, 141.

Shimizu, R., and Ogasawara, Y. (2013) Diversity of potassium-bearing tourmalines in diamondiferous Kokchetav UHP metamorphic rocks: A geochemical recorder from peak to retrograde metamorphic stages. Journal of Asian Earth Sciences, 63, 39-55.

Skogby, H., Bosi, F., and Lazor, P. (2012) Short-range order in tourmaline: a vibrational spectroscopic approach to elbaite. Physics and Chemistry of Minerals, 39, 811-816.

Van Hinsberg, V.J., Henry, D.J., and Dutrow, B.L. (2011) Tourmaline as a petrologic forensic mineral: A unique recorder of its geologic past. Elements, 7, 327-332.

Von Goerne, G., and Franz, G. (2000) Synthesis of Ca-tourmaline in the system CaO-MgO-Al_2O_3-SiO_2-B_2O_3-H_2O-HCl. Mineralogy and Petrology, 69, 161-182.

Watenphul, A., Wunder, B., and Heinrich, W. (2009) High-pressure ammonium-bearing silicates: Implications for nitrogen and hydrogen storage in Earth´s mantle. American Mineralogist, 94, 283-292.

Werding, G., and Schreyer, W. (1984) Alkali-free tourmaline in the system MgO-Al_2O_3-B_2O_3-SiO_2-H_2O. Geochimica et Cosmochimica Acta, 48, 1331-1344.

Williams, L.B., Wilcoxon, B.R., Ferrell, R.E., and Sassen, R. (1992) Diagenesis of ammonium during hydrocarbon maturation and migration. Wilcox Group, Louisiana, U.S.A. Applied Geochemistry, 7, 123-134.

Willner, A.P., Rötzler, K., and Maresch, W.V. (1997) Pressure-temperature and fluid evolution and quartzo-feldspathic metamorphic rocks with a relic high-pressure,

granulite-facies history from the Central Erzgebirge. Journal of Petrology, 38, 307-336.

Wunder, B., Meixner, A., Romer, R.L., Wirth, R., and Heinrich, W. (2005) The geochemical cycle of boron: Constraints from boron isotope partitioning experiments between mica and fluid. Lithos, 84, 206-216.

Žáček, V., Jiří, F., Petrov, A., and Hyršl, J. (2000) Tourmalines of the povondraite-(oxy)dravite series from the cap rock of meta-evaporite in Alto Chapare, Cochabamba, Bolivia. Journal of the Czech Geological Society, 45, 3-12.

Table captions

TABLE 1. Assignment of observed IR-bands for NH_4-tourmaline.

TABLE 2. Chemical composition of NH_4-bearing tourmaline determined by EMP.

TABLE 3. EMP-determined chemical composition of natural tourmalines from the high *P*/ low *T* mica schist unit, Erzgebirge.

Figure captions

FIGURE 1. Plot of tourmaline cell dimensions *c* versus *a* for dravite, K-bearing tourmaline, Mg-foitite and NH_4-bearing tourmaline presented in this study. Error-bars are smaller than symbol size.

561 **FIGURE 2.** SEM photomicrograph of the run products. Large prismatic crystals are NH_4-
562 bearing tourmaline, platy crystals with hexagonal shape are phengite, fine grained material
563 comprises also of traces of coesite as determined from XRD analyses.
564
565 **FIGURE 3**. IR spectrum of NH_4-bearing tourmaline in the range 4000 to 500 cm^{-1} taken from a
566 thin film of the synthetic tourmaline. For comparision an IR spectrum of natural schorl
567 (Salisbury et al. 1991) is shown. Assignment of the bands is given in Table 1.
568

TABLE 1. Assignment of observed IR-bands for NH_4-bearing tourmaline.

Mode	wavenumber (cm^{-1})	assignment	references
ν1	3650	OH-stretching $^{[X]}\square$-O1H	Fantini et al. (2014)
ν2	3608	OH-stretching $^{[Y]}Al(Mg)\,^{[Y]}Al^{[Y]}Al$-O1H	Schreyer et al. (2000)
ν3	3551	OH-stretching $^{[Y]}Mg^{[Z]}Al^{[Z]}Al$-O3H	Gonzales-Carreño et al. (1988)
ν4	3473	OH-stretching $^{[Y]}Al^{[Z]}Al^{[Z]}Al$-O3H	Skogby et al. (2012)
ν5	3320	N-H-stretching	Busigny et al. (2003b)
ν6	3060	N-H-stretching	Busigny et al. (2003b)
ν7	1460	N-H-bending	Busigny et al. (2003b)
ν8	1420	N-H-bending	Busigny et al. (2003b)
ν9	1370	N-H-bending	Busigny et al. (2003b)
ν10	1340	B-O-stretching	Jagannada Reddy et al. (2007)
ν11	1282	B-O-stretching	Jagannada Reddy et al. (2007)
ν12	1105	Mg-OH-bending	Jagannada Reddy et al. (2007)
ν13	1030	Si-O-stretching	Jagannada Reddy et al. (2007)
ν14	790	B-O-bending	Jagannada Reddy et al. (2007)
ν15	760	Si-O-bending	Jagannada Reddy et al. (2007)
ν16	710	"breathing" of bridging oxygens in Si-O rings	Jagannada Reddy et al. (2007)

TABLE 2. Chemical composition of synthetic NH_4-bearing tourmaline determined by EMP.

Standard	nat. NH_4-Phg
No of analyses	49
$(NH_4)_2O$	0.22(0.03)
SiO_2	38.57(0.85)
Al_2O_3	35.96(0.67)
MgO	9.71(0.38)
Total	84.47(1.23)
NH_4	0.08(0.01)
Si	6.07(0.06)
Al	6.65(0.07)
Mg	2.28(0.08)

Structural formula:
$^{[X]}((NH_4)_{0.08(1)}\square_{0.92(1)})^{[Y]}(Mg_{2.28(8)}Al_{0.72(8)})$
$^{[Z]}(Al_{5.93(6)}Si_{0.07(6)})^{[T]}(Si_{6.00(5)}O_{18})(BO_3)_3(OH)_4$.

Analyses are given in wt%. Cations are calculated on 15 (Si + Al + Mg) and assuming 3 B pfu. 1σ-standard deviations are given in parentheses. Abbreviations: nat. NH_4-Phg: natural NH_4-bearing phengite.

TABLE 3. EMP-determined chemical composition of natural tourmalines from the high *P*/ low *T* mica schist unit, Erzgebirge.

	Tur1	Tur2	Tur3
No of analyses	5	5	5
$(NH_4)_2O$	0.20(0.02)	0.21(0.02)	0.19(0.02)
Na_2O	2.13(0.19)	2.34(0.06)	2.19(0.19)
CaO	0.06(0.01)	0.06(0.01)	0.07(0.01)
K_2O	0.03(0.01)	0.03(0.01)	0.03(0.01)
SiO_2	37.00(0.16)	37.09(0.23)	36.83(0.10)
Al_2O_3	30.41(0.59)	29.83(0.19)	30.27(0.71)
MgO	6.36(0.42)	7.11(0.08)	6.61(0.59)
FeO	8.18(0.25)	7.84(0.19)	8.03(0.35)
TiO_2	0.79(0.24)	0.72(0.05)	0.66(0.08)
F	0.20(0.08)	0.27(0.04)	0.24(0.08)
Total	85.38(0.11)	85.52(0.48)	85.13(0.15)
NH_4	0.08(0.01)	0.08(0.01)	0.07(0.01)
Na	0.69(0.06)	0.76(0.02)	0.71(0.06)
Ca	0.01(0.00)	0.01(0.00)	0.01(0.00)
K	0.01(0.00)	0.01(0.00)	0.01(0.00)
Si	6.18(0.02)	6.19(0.03)	6.17(0.01)
Al	5.99(0.10)	5.86(0.04)	5.97(0.13)
Mg	1.58(0.11)	1.77(0.02)	1.65(0.15)
Fe	1.14(0.03)	1.09(0.02)	1.12(0.05)
Ti	0.10(0.03)	0.09(0.01)	0.08(0.01)
F	0.01(0.00)	0.01(0.00)	0.01(0.00)

Mean tourmaline formula:

$^{[X]}((NH_4)_{0.08(1)}Na_{0.72(5)}Ca_{0.01(0)}K_{0.01(0)}\square_{0.18(5)})$

$^{[Y]}(Mg_{1.67(9)}Fe_{1.12(3)}Al_{0.21(9)})$

$^{[Z]}(Al_{5.73(9)}Ti_{0.09(2)}Si_{0.18(2)})^{[T]}(Si_{6.00(2)}O_{18})(BO_3)_3$

$^{[V]}(OH)_{3.00(3)}{}^{[W]}((OH)_{0.68(3)}O_{0.31(4)}F_{0.01(0)})$

Analyses (given in wt%) for three tourmaline from sample # 61 after Mingram and Bräuer (2001) using natural NH_4-phengite as N-standard. Formula are calculated for 15 cations on (Y, Z, T)-positions and assuming 3 B pfu. 1σ-standard deviations are given in parentheses.

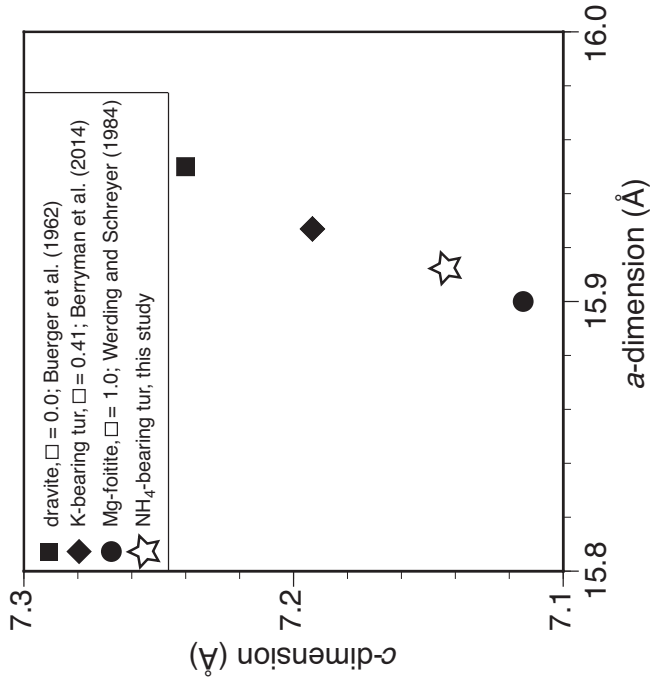
dravite, □ = 0.0; Buerger et al. (1962)
K-bearing tur, □ = 0.41; Berryman et al. (2014)
Mg-foitite, □ = 1.0; Werding and Schreyer (1984)
NH4-bearing tur, this study
7.3
7.2
7.1
c-dimension (Å)
15.8
15.9
16.0
a-dimension (Å)


5 µm

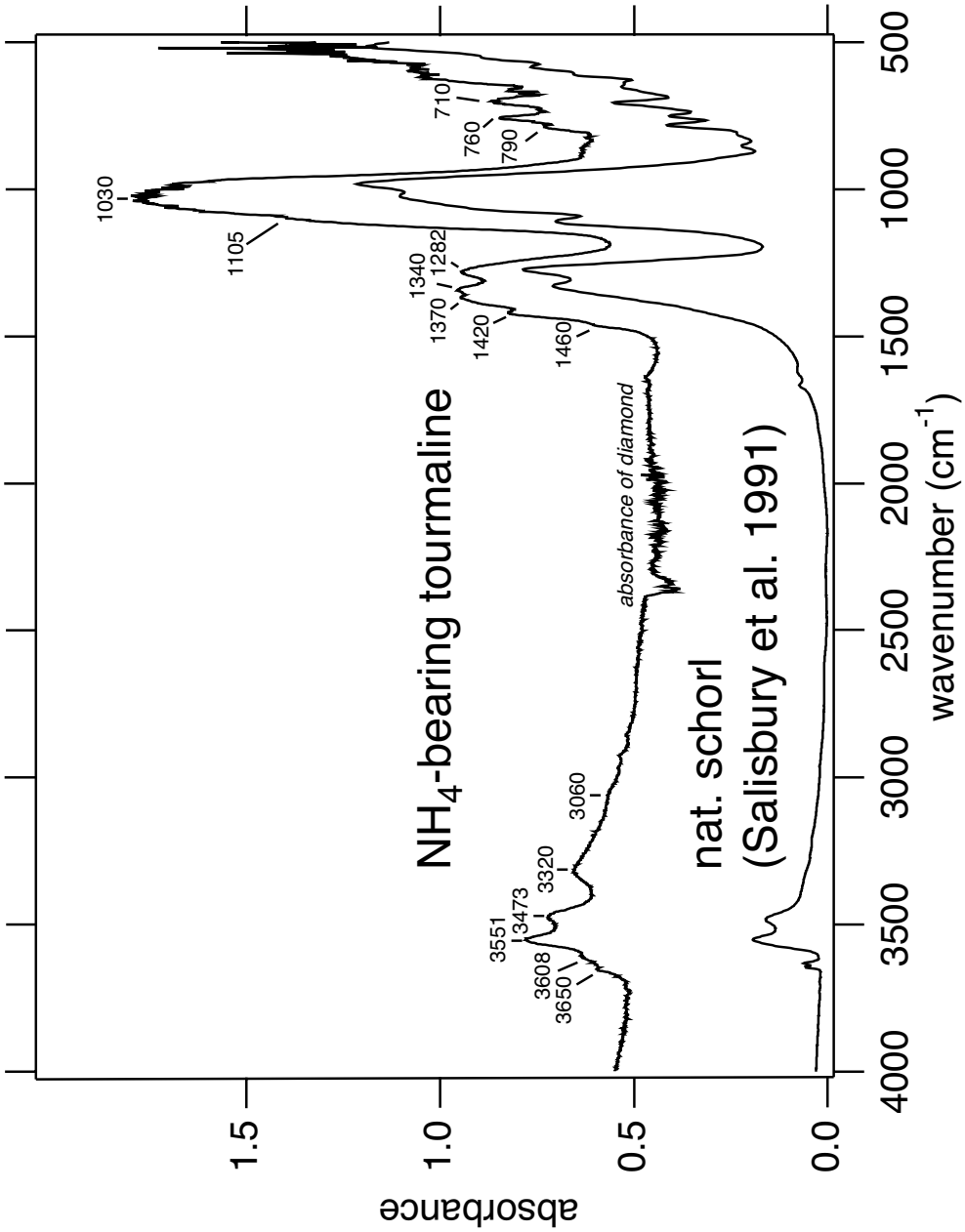
absorbance
1.5
1.0
0.5
0.0
4000
3500
3000
2500
2000
1500
1000
500
wavenumber (cm-1)
NH4-bearing tourmaline
nat. schorl
(Salisbury et al. 1991)
absorbance of diamond
1030
1105
710
760
790
1340
1282
1370
1420
1460
3060
3320
3551
3473
3608
3650